

A Ku-Band Filtering Duplex Antenna for Satellite Communications

Mostafa G. Aly^{1,*}, Chunxu Mao², Steven Gao³, and Yi Wang⁴

Abstract—In this paper, a dual-polarisation shared-aperture duplex antenna is presented for satellite communications at the standard microwave Ku-band, based on the integrated filtering-antenna concept and co-design approach. The design relies on the use of resonators coupled to the radiating dual-band dual-polarisation antenna. The resonant patch antenna forms one pole of each channel filter, resulting in a third-order filter in the Rx channel and a second-order filter in the Tx channel. The Rx and Tx ports of the antenna take in horizontal and vertical linear polarisations, respectively. The integrated duplexer helps to increase the isolation between the ports and the selectivity of each channel. The integration between the filter and the antenna is achieved by electromagnetic coupling, without the need of external matching circuits. Thus it attains a compact footprint. The operation frequencies of the demonstrated duplex antenna are from 11 to 12.5 GHz (12.8%) for the downlink to the Rx port, and from 13 to 14.4 GHz (10.2%) for the uplink at the Tx port. High port-to-port isolation of over 40 dB is realized to reduce channel interference. Flat in-band average gains are achieved to be 7.8 and 8.3 dBi, for the low- and high-bands, respectively.

1. INTRODUCTION

Highly integrated radio frequency (RF) modules with a compact size and multiple functions are of great interest for modern wireless communication applications, due to the constant demands for size and cost reduction of RF systems. The integration of passive components, such as filters, power dividers, duplexers, and antennas in the RF front-end, has attracted enormous research interests in the past several years.

Wireless communication applications, in particular satellite communications, have experienced rapid development in the past decade. At a ground station, a duplexing and dual-polarisation transceiver front-end, as illustrated in Fig. 1, has been widely used. Taking a standard Ku-band system as an example, the receiver (Rx) channel and transmitter (Tx) channel not only are duplexing but also take in different polarisations. Traditionally, the dual-polarisation antenna, either a shared aperture or sometimes two separate apertures, and the duplexer are separately designed to match a system impedance of $50\ \Omega$ and then cascaded together through $50\ \Omega$ interfaces. An integrated duplex antenna module can be an attractive alternative, where the antenna and duplexer are co-designed to form an inseparable component with two ports and one radiator. The elimination of $50\ \Omega$ interconnections makes the antenna-duplexer module more compact. It also avoids the potential multiple reflections between the connectors. The orthogonal polarisation between the two ports and the duplexer together ensure high isolation between the two channels so as to reduce their interference.

Several planar duplex antennas with compact sizes have been reported in literature. These can be realized by two cascaded triplet sections of quarter wavelength resonators [1], by coupling electromagnetic (EM) waves through dog-bone-shape slotted ground [2], or by microstrip-to-slot

Received 15 July 2019, Accepted 13 August 2019, Scheduled 14 September 2019

* Corresponding author: Mostafa Gamal Aly (M.G.Aly@greenwich.ac.uk).

¹ Faculty of Engineering and Science, University of Greenwich, ME4 4TB, UK. ² Department of Electrical Engineering, Pennsylvania State University, USA. ³ School of Engineering and Digital Arts, University of Kent, CT2 7NZ, UK. ⁴ Department of Electronic Electrical and Systems Engineering, University of Birmingham, B15 2TT, UK.

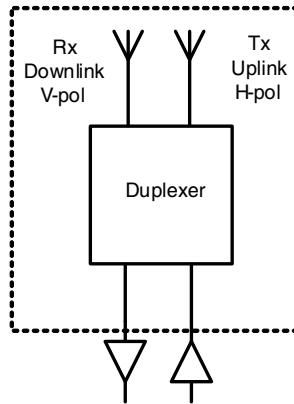


Figure 1. Block diagram of the proposed duplex antenna.

transition technique [3], to name just a few. T-shaped probes presented in [4] acted as a two-pole band-pass filter (BPF) in a duplex patch antenna, whereas two H-shaped feed-lines aided in achieving a quasi-elliptic BPF in [5]. Tuneable capacitors were also used to control the resonating frequencies of two planar inverted-F antennas (PIFAs), resulting in tuneable duplexing antenna transceivers [6]. A compact duplexer antenna was achieved in [7] using a stub-loaded resonator that operated at two resonant frequencies to match two sets of split-ring resonators.

Filtering antennas have been studied for its compact size, enhanced bandwidth, frequency selectivity, high port isolation, and flat in-band gain [8,9]. Filtering antennas could be achieved by cascading the radiating element after the filter stage, such as the gamma-shaped antenna [10,11], a circular patch with annular ring [12], and a rectangular patch antenna [13]. An edge coupled filtering antenna in [14] relied on bending the filter structure 180 degree, and coupling each branch to the other. Antenna-filter-antenna is another technique to achieve the filtering antenna concept [15]. Back-to-back microstrip patch antennas acted as resonators as well as radiators when being coupled to a slotted ground plane in between [16,17]. Cavity resonators were also used to play the filter role [18]. Dual-band notches were introduced in [19], by adding a band stop filter at the feed-line.

In this paper, a filtering duplex antenna is proposed for the satellite communications within the microwave Ku-band. The duplex antenna is composed of two sets of resonators and a dual-polarisation patch antenna. The integrated system depends on EM coupling through the slotted ground plane, without the need of $50\ \Omega$ interconnections and matching networks. Compared to conventional cascaded duplexer antenna, the proposed filtering duplex system not only makes the RF front-end much more compact, but also improves the frequency response of the overall system. That is due to reduced mismatch and the elimination of multi-reflection between the duplexer and the radiating elements [20].

The integrated design methodology will be described in Section 2. Section 3 discusses the design of the planar duplexer. The microstrip antenna is discussed in Section 4. The integrated duplex antenna is elaborated in Section 5. All simulations are carried out using Computer Simulation Technology (CST) Microwave Studio. Section 6 reports the simulated and measurement results. Section 7 concludes the paper.

2. INTEGRATED CONFIGURATION AND DESIGN METHOD

The conventional cascaded duplex system, as in Fig. 2(a), consists of two ports for transmitter and receiver, a duplexer, an antenna, and the matching circuit. Mostly, a broadband antenna is used to cover both uplink and downlink frequency bands. In some cases, multiband antennas or multiple antennas are used as well. Traditionally, the antenna and duplexer are designed separately and cascaded via $50\ \Omega$ interfaces. This leads to mismatching between RF components, extra circuit areas for the interconnection, and a relatively large component-count of the front-end. On the other hand, the integrated duplex antenna architecture is shown in Fig. 2(b). In this system, the duplexer and radiating element are integrated into a single device, combining the functions of duplexer, filter, and antenna.

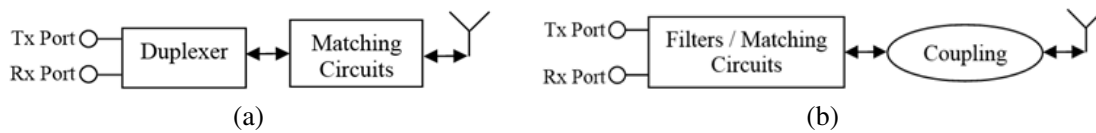


Figure 2. Block diagram of (a) traditional cascaded system (b) integrated duplex antenna subsystem.

Consequently, the component number and therefore the volume and cost are significantly reduced. Besides, the losses associated with the matching circuit can be removed.

To achieve the duplex antenna, a design concept based on coupled resonators and dual-mode resonant antenna is proposed, with the topology as shown in Fig. 3. The antenna has two resonant modes at f_1 and f_2 , and in this case they are orthogonally polarised. These are coupled to the two channels respectively. The transmitting path consists of one resonator in addition to the radiating element itself, both resonating at f_2 . This essentially forms a second-order filter. The receiving path contains two resonators and the antenna all resonating at f_1 , and therefore a third-order filter response is achieved. Finally, the port isolation is achieved by having the coupling line of the Tx port facing the opposite side of the substrate away from the Rx one, and also by introducing a separating distance in between. These two features result in having a significant isolation between ports, as referred to by the path of resonators shown in Fig. 3. It is important to note that the order of the filters (third and second order in this case) is mainly determined by the requirements in terms of channel bandwidth and isolation.

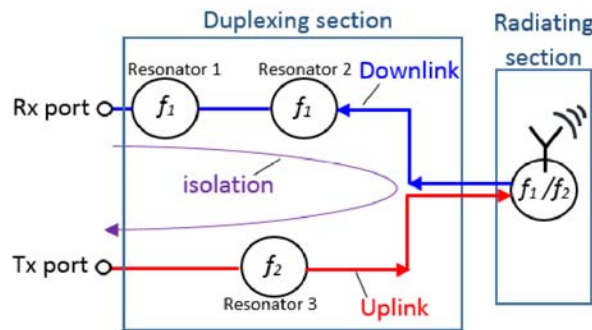


Figure 3. Topology of the integrated filtering duplex antenna.

The duplex antenna is formed of coupled resonators without the use of separated duplexers, antennas, and interconnection matching networks. This effectively forms a multiport filtering network with all of the resonators and radiating elements contributing to the bandwidth and frequency selectivity. For the purpose of satellite communications, this design targets the downlink and uplink frequency bands to have a return loss bandwidth (RLBW) from 11 to 12.5 GHz (12.8%) and from 13 to 14.4 GHz (10.2%), respectively, operating within the standard Ku-band.

In most cases, circularly polarised antennas are preferred for satellite communication applications due to their unfixed orientation flexibility feature. However, accomplishing a dual-linear-polarised integrated design may also benefit in some niche applications when the broadcasting satellite is fixed. Isolation is increased by the usage of an orthogonal polarisation in the case of receiving a dominant interference [21]. Moreover, linear polarisation is not affected by atmospheric conditions, particularly at the higher frequency bands [22].

3. PLANAR DUPLEXER

The coupling between the added resonators and the radiating element is responsible for the increase of the operating bandwidth. The coupled-resonator filter design approach [23] was adopted to realise the return loss (RL) of +20 dB for both bands. For the targeted fractional bandwidth (FBW) at the

low-band (12.8%) in a 2nd-order filtering circuit, the g -element values were found to be $g_1 = 1.4029$, $g_2 = 0.7071$ and $g_3 = 1.9841$. And for the high-band (10.2%), a 1st-order filtering circuit is used, and the g -element values were found to be $g_1 = 0.6986$ and $g_2 = 1$. These values are translated to coupling coefficients and external quality factors using Eqs. (1) and (2) [23]:

$$M_{i,i+1} = \frac{\text{FBW}}{\sqrt{g_i \cdot g_{i+1}}} \quad (1)$$

$$Q_{en} = \frac{g_n \cdot g_{n+1}}{\text{FBW}} \quad (2)$$

For the first-order transmitting channel with the central frequency $f_2 = 13.7$ GHz, and FBW of 0.102, the coupling coefficient is obtained as $M_{12} = 0.122$, and the external quality factor is $Q_{e1} = 6.85$. For the second-order receiving channel with the central frequency $f_1 = 11.75$ GHz and FBW of 0.128, the coupling coefficients are obtained as $M_{12} = 0.1285$, $M_{23} = 0.1081$, and the external quality factors are $Q_{e1} = 7.75$ and $Q_{e2} = 10.961$.

These obtained values are then used in the initial dimensioning of the circuit layout. It should be noted that the initial dimensions only provide a starting point for the optimization. The resonant characteristics of the radiating element are very different from the microstrip line resonator in terms of quality factor. For this reason, the dimensions extracted from M and Q_{ex} are not as accurate and reliable as in the design of conventional microstrip filters. Thus extensive parameter study and optimizations were further required.

4. DUAL-BAND DUAL-POLARISATION MICROSTRIP ANTENNA

As mentioned in Section 1, a broadband antenna or a multiband one is required to act as the radiating element covering both operating channels in a duplex antenna. Nonetheless, for having an integrated design, it is preferable to have a single unidirectional antenna, operating at dual-band with orthogonal polarisations. This would benefit in reducing coupling and improving diversity to combat fading and co-channel interference [24]. The configuration of the proposed dual-band dual-polarisation rectangular patch is as shown in Fig. 4. It consists of two substrates of Rogers RO4003C with 3.55 dielectric constant and 0.2 mm thickness. The patch is printed on top of the first substrate. For the second substrate, the slotted ground plane is etched on the top, while both of the microstrip feed-lines are printed on the lower face. The presence of such a slotted ground plane helped in coupling the EM waves to the patch antenna. The dimensions of the rectangular patch are deduced using Eq. (3), the dominant mode with the lowest frequency (11 GHz), and Eq. (4) which is the second mode with the highest frequency

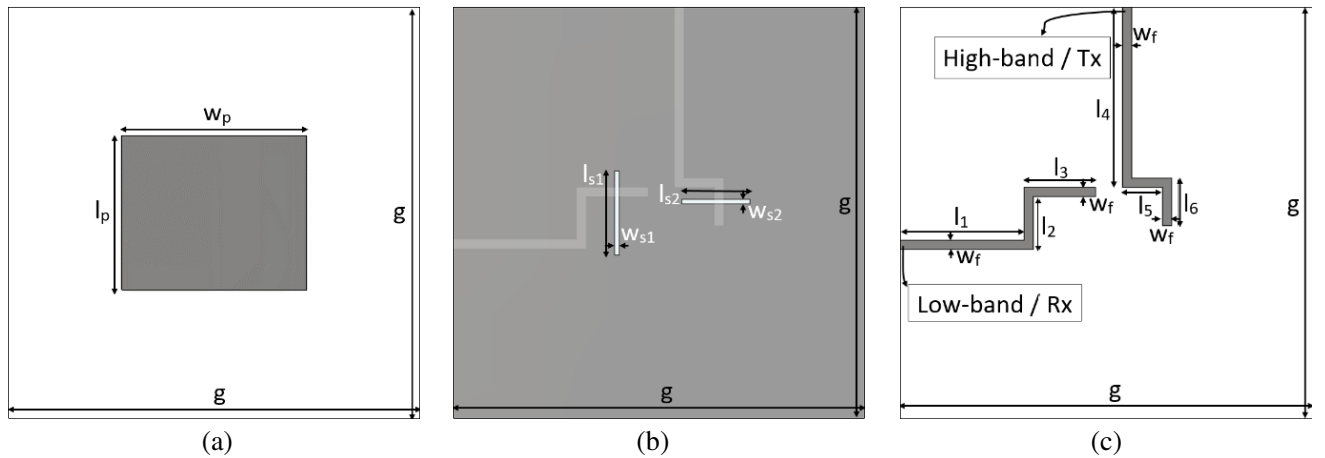


Figure 4. Layout of the dual-polarisation antenna. (a) Rectangular patch. (b) Slotted-ground plane. (c) Two feed-lines.

(14.5 GHz) [22]:

$$(f_r)_{001} = \frac{c}{2W\sqrt{\epsilon_r}} \quad (3)$$

$$(f_r)_{010} = \frac{c}{2L\sqrt{\epsilon_r}} \quad (4)$$

where c is the speed of light, and ϵ_r is the relative permittivity of the substrate. The design parameters are listed in Table 1. Such a design had the dual-band response displayed in Fig. 5. The low and high-band resonances occurred at 11.4 and 13.3 GHz, respectively. Overall port isolation was obtained to be 38.4 dB. It is worth mentioning that the patch operates at two orthogonal linear polarizations, horizontal for the low-band, and vertical for the high-band. The dual-polarisation operation will be clarified further in the coming section.

Table 1. Parameters of the proposed dual-band dual-polarisation antenna (unit: mm).

g	l_p	w_p	l_{s1}	w_{s1}	l_{s2}	w_{s2}
20	7.5	9	4.1	0.23	3.3	0.25
w_f	l_1	l_2	l_3	l_4	l_5	l_6
0.45	6	2.55	3.45	8.75	1.95	2.3

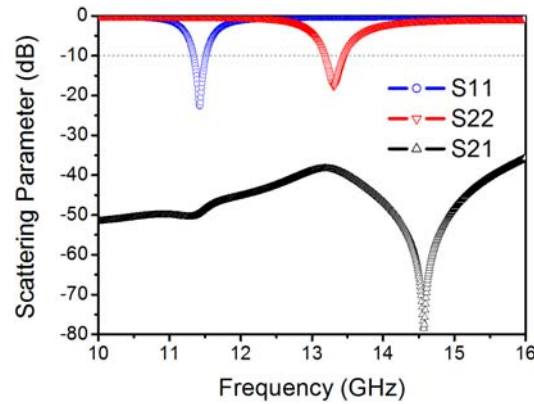


Figure 5. Simulated dual-band antenna response.

5. INTEGRATED FILTERING DUPLEX ANTENNA

The configuration of the integrated filtering duplex antenna is shown in Fig. 6, and the geometric parameters are recorded in Table 2. The integrated design is achieved onto two substrates of the same dielectric material Rogers RO4003C with the same specifications. Again the patch is printed on top of the first substrate, while for the second substrate, the slotted ground plane is etched on the top, and the channel resonators and feed-lines are printed on the lower face. The filtering duplex antenna is realised by electromagnetically coupling the last resonator in the two channels to the two polarisations of the antenna respectively. This results in a highly integrated and compact design in which the duplexing and radiating elements become inseparable. To achieve the impedance matching performance at both bands, the centre frequencies for the two channels of the duplexer and the dual-band antenna were set to be matched. Then by tuning the coupling strength between resonators, good impedance matching performance can be realised. It should be noted that the separating distance s_3 plays an important role in controlling the isolation between both ports. As a result, the simulated surface current distribution of the integrated design is of two linear polarisations, horizontal at the centre frequency of the low-band and vertical at that of the high-band. This can be seen in Fig. 7. The filtering duplex antenna has three

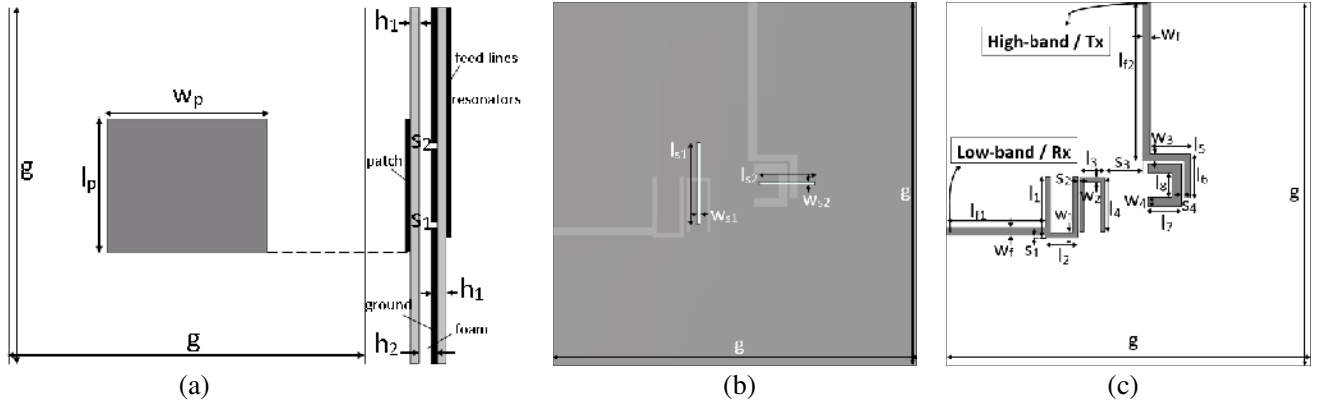


Figure 6. Integrated filtering duplex antenna: (a) Dual-band patch. (b) Side view. (c) Slotted-ground plane. (d) Feeding network.

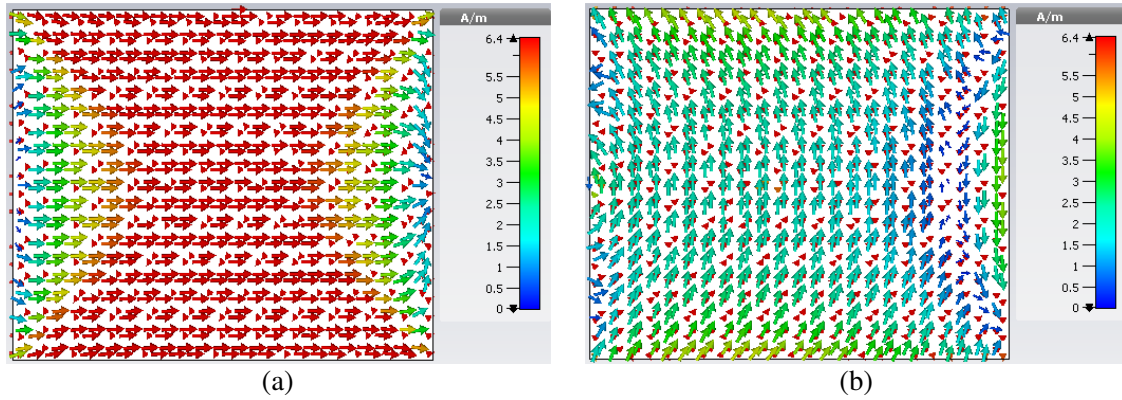


Figure 7. Simulated current distribution on the antenna patch at (a) 11.7 GHz (b) 13.75 GHz.

Table 2. Parameters of the proposed integrated design (unit: mm).

g	h₁	h₂	l_p	w_p	l_{s1}	w_{s1}	l_{s2}	w_{s2}
20	1	0.2	7.5	9	3.1	0.19	4	0.32
l_{f1}	l_{f2}	w_f	l₁	w₁	l₂	l₃	w₂	l₄
5.46	8.75	0.45	3.4	0.27	1.7	1.36	0.2	2.97
s₁	s₂	s₃	s₄	l₅	l₆	w₃	l₇	l₈
0.2	0.12	2.61	0.16	2.2	2.4	0.36	1.84	1.35

resonance poles for the low-band and two for the high-band, including the resonance of the radiating patch at both. Eventually, this forms a five-pole filtering network as shown in Fig. 9(a). The simulated downlink bandwidth is from 11 to 12.5 GHz (12.8%), while that of the uplink is from 13 to 14.4 GHz (10.2%). The simulated overall port isolation is 41 dB.

6. SIMULATIONS AND MEASUREMENTS

A prototype of the design was fabricated as shown in Fig. 8 and tested. The measured scattering parameters are compared to the simulated ones in Fig. 9(a). Measurements were conducted using an Agilent Network Analyzer N5230A. A good agreement was achieved between the results, having the

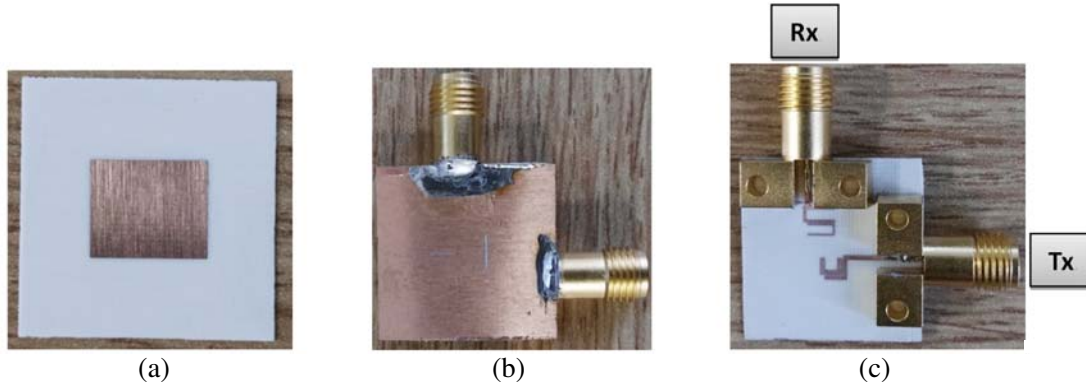


Figure 8. Fabricated prototype: (a) Dual-band patch. (b) Slotted-ground plane. (c) Feeding network.

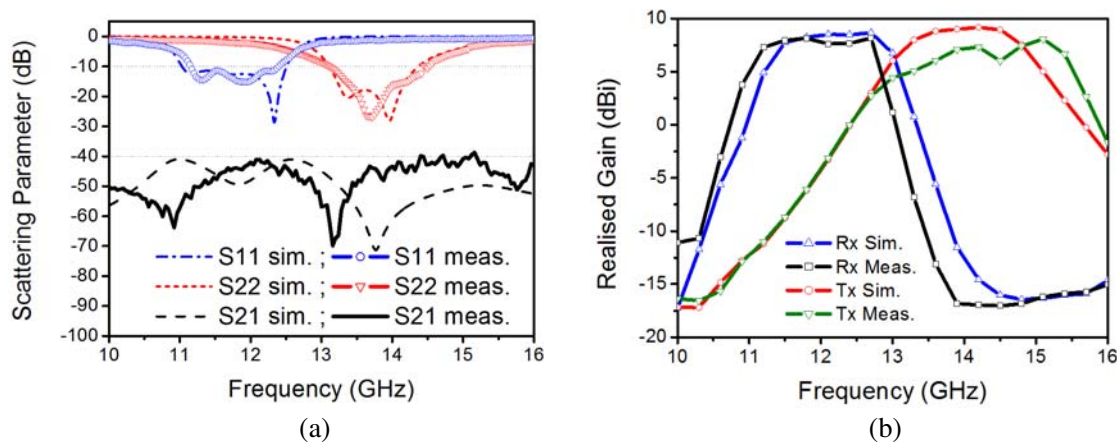


Figure 9. Filtering duplex antenna; simulated versus measured: (a) Scattering parameters. (b) Realised gains.

Table 3. Comparison of filtering duplex antenna performance.

Ref.	Pol. Type	f_1, f_2 (GHz)	RLBW (%)	Isolation (dB)	Avg. Gain (dBi)
[2]	Single	2.45, 5.25	5.3, 5.7	20	3
[4]	Single	2.06, 2.6	10.6, 6.9	45	3.4
[5]	Dual	1.94, 2.6	23, 8	35	8.5
[7]	Single	2.6, 2.9	5, 4.2	32	4.75
This work	Dual	11.75, 13.75	10.95, 10.9	40	8.1

low-band of three reflection dips over the frequency range from 11.14 to 12.43 GHz (10.95%), and the high-band of two matching points over the range from 13 to 14.5 GHz (10.9%). The measured overall isolation between ports is better than 39.6 dB. The prototype device used very thin substrates with a small footprint, which makes it sensitive to the assembly. The relatively large connectors also have some effect on the feeding circuitry. These are believed to be the main causes for the small discrepancy between the measurements and simulations. Fig. 9(b) displays the in-band gains as a function of frequency, which recorded a simulated average of 7.8 and 8.3 dBi, and a measured average of 7.7 and 6 dBi, for the low and high bands, respectively. The discrepancy at the Tx port gain is believed to be

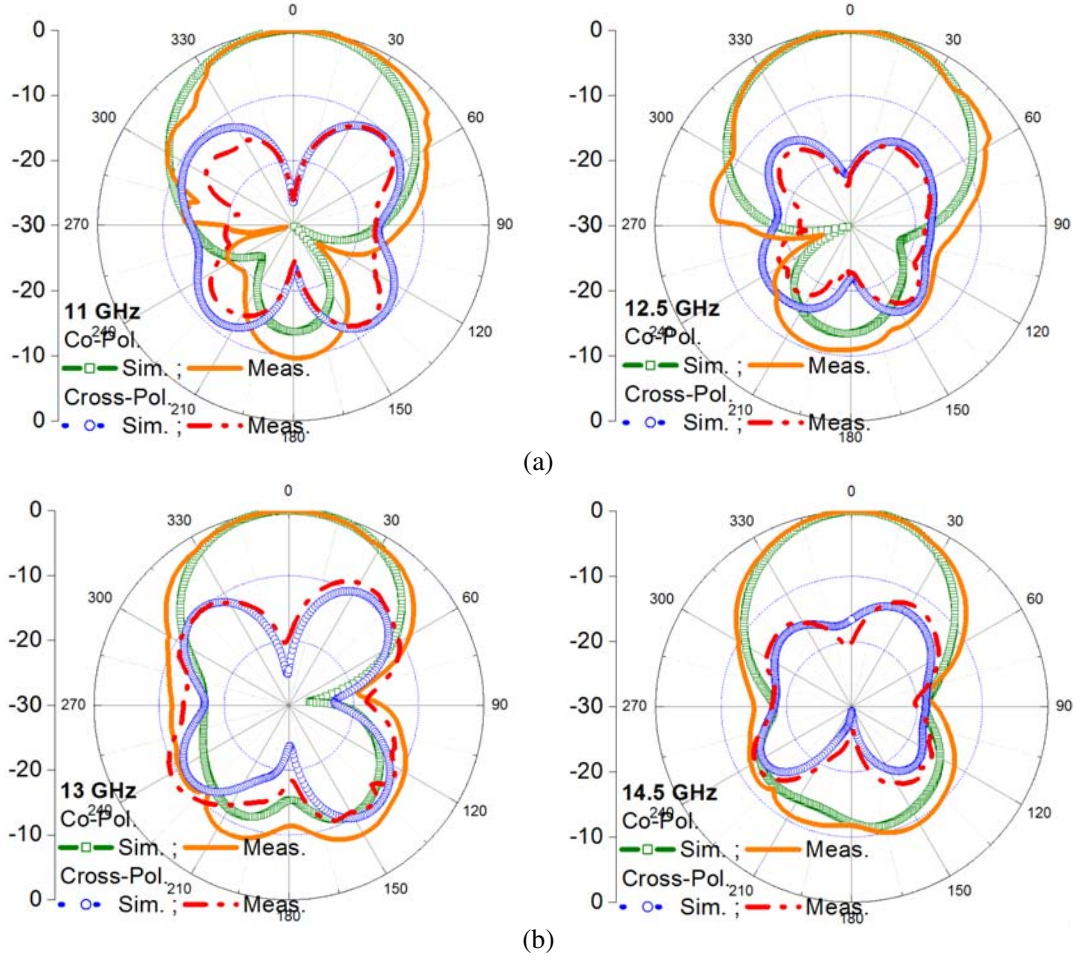


Figure 10. Simulated versus measured radiation patterns (co and cross polarisations) at: (a) The low band. (b) The high band.

mainly due to being over sensitive to the cables in the measuring set-up at the high frequencies. Fig. 10 compares between the simulated and measured radiation patterns for both co- and cross-polarisations, at the low and high bands, with good agreement achieved. It is worth mentioning that both of radiation patterns and gain measurements were taken under the supervision of the National Telecommunication Institute in Egypt.

7. CONCLUSION

In this paper, a novel integrated filtering duplex antenna was proposed for the satellite communication applications. The design methodology of integrating the duplexer to the dual-band patch antennas was presented. To prove the concept, an integrated filtering duplex antenna was realised by coupling the duplexer to the dual-band patch via EM waves. This removed the need of interconnection and matching network between the duplexer and antenna, as in traditional systems. The frequency responses, such as bandwidth and frequency selectivity, are controlled by the coupling between the resonators and the radiating patch. The simulated results agree well with the measured ones, showing a good performance in terms of impedance matching, isolation, realised gains, and radiation patterns. The integrated prototype proves to have flat in-band gains with directional radiation patterns. Another advantage of such an integrated design is the high isolation achieved between the two ports, resulting in channel interference reduction. And that is proved in the comparison introduced in Table 3, presenting the polarisation type, centre frequencies of the dual-band operation, the impedance bandwidth, the port

isolation, and finally the average gain of each design. This highly integrated design renders compact footprint, which makes it useful for RF front-end applications serving satellite communications at the Ku-band.

ACKNOWLEDGMENT

Mostafa G Aly is grateful to the funding provided by Modern Sciences & Arts University, Egypt.

REFERENCES

1. Chen, F., H. Hu, J. Qiu, M. Guo, and Q. Chu, "Novel diplexer with improved isolation using asymmetric transmission zeros technique," *Chinese J. Electron.*, Vol. 25, No. 3, 591–594, 2016.
2. Lee, Y. J., J. H. Tarng, and S. J. Chung, "A filtering diplexing antenna for dual-band operation with similar radiation patterns and low cross-polarization levels," *IEEE Antennas Wirel. Propag. Lett.*, Vol. 16, 58–61, 2017.
3. Cheong, P., K. F. Chang, W. W. Choi, and K. W. Tam, "A highly integrated antenna-triplexer with simultaneous three-port isolations based on multi-mode excitation," *IEEE Trans. Antennas Propag.*, Vol. 63, No. 1, 363–368, 2015.
4. Lin, X., Z.-M. Xie, P.-S. Zhang, and Y. Zhang, "Broadband filtering duplex patch antenna with high isolation," *IEEE Antennas Wirel. Propag. Lett.*, Vol. PP, No. 99, 2017.
5. Duan, W., X. Y. Zhang, Y.-M. Pan, J.-X. Xu, and Q. Xue, "Dual-polarized filtering antenna with high selectivity and low cross polarization," *IEEE Trans. Antennas Propag.*, Vol. 64, No. 10, 4188–4196, 2016.
6. De Luis, J. R., A. Morris, Q. Gu, and F. De Flaviis, "Tunable duplexing antenna system for wireless transceivers," *IEEE Trans. Antennas Propag.*, Vol. 60, No. 11, 5484–5487, 2012.
7. Mao, C. X., S. Gao, Y. Wang, F. Qin, and Q. X. Chu, "Compact highly integrated planar duplex antenna for wireless communications," *IEEE Trans. Microw. Theory Tech.*, Vol. 64, No. 7, 2006–2013, 2016.
8. Zayniyev, D. and D. Budimir, "An integrated antenna-filter with harmonic rejection," *3rd Eur. Conf. Antennas Propag.*, 393–394, 2009.
9. Chen, C. F., T. Y. Huang, C. P. Chou, and R. B. Wu, "Microstrip diplexers design with common resonator sections for compact size, but high isolation," *IEEE Trans. Microw. Theory Tech.*, Vol. 54, No. 5, 1945–1952, 2006.
10. Wu, W. J., Y. Z. Yin, S. L. Zuo, Z. Y. Zhang, and J. J. Xie, "A new compact filter-antenna for modern wireless communication systems," *IEEE Antennas Wirel. Propag. Lett.*, Vol. 10, 1131–1134, 2011.
11. Wu, W., C. Wang, X. Wang, and Q. Liu, "Design of a compact filter-antenna using dgs structure for modern wireless communication systems," *IEEE Int. Symp. Microwave, Antenna, Propag. EMC Technol. Wirel. Commun.*, 355–358, 2013.
12. Wu, W., J. Wang, R. Fan, and Q. Zhang, "A broadband low profile microstrip filter-antenna with an omni-directional pattern," *Asia-Pacific Conf. Antennas Propag.*, 580–582, 2014.
13. Shang, X. and M. J. Lancaster, "Patch antenna with integrated bandpass filter," *4th Annu. Semin. Passiv. RF Microw. Components*, 1–5, 2013.
14. Kang, C., H. Zhang, Y. Wang, and L. Xu, "A new compact edge coupled filter-antenna," *Int. Symp. Antennas, Propag. EM Theory*, 115–117, 2016.
15. Liao, C., Y. Lin, C. Chen, S. Kao, and H. Chen, "A novel aperture-coupled circularly polarized square-ring patch antenna for wireless communication systems," *IEEE 5th Asia-Pacific Conf. Antennas Propag.*, 57–58, 2016.
16. Kaouach, H. and A. Kabashi, "Antenna-filter-antenna based frequency selective surfaces for quasi-optical applications in Q-band," *Int. Work. Antenna Technol.*, 1–4, 2015.

17. Naseri, P., F. Khosravi, and P. Mousavi, "Antenna-filter-antenna-based transmit-array for circular-polarization application," *IEEE Antennas Wirel. Propag. Lett.*, Vol. 1225, 2016.
18. Li, T., H. Cheng, and X. Gong, "Integrated single-fed circularly-polarized patch antennas with high-Q cavity filters," *IEEE Antennas Propag. Soc. Int. Symp.*, 1873–1874, 2014.
19. Liu, Q., C. Yu, X. Wu, Z. Zhang, and S. Wang, "A novel design of dual-band microstrip filter antenna," *IEEE Adv. Inf. Manag. Commun. Electron. Autom. Control Conf.*, 1573–1576, 2016.
20. Shang, X., Y. Wang, W. Xia, and M. J. Lancaster, "Novel multiplexer topologies based on all-resonator structures," *IEEE Trans. Microw. Theory Tech.*, Vol. 61, No. 11, 3838–3845, 2013.
21. Wong, K., *Compact and Broadband Microstrip Antennas*, Vol. 3, John Wiley & Sons, New York, 2002.
22. Balanis, C. A., *Antenna Theory Analysis and Design*, 3rd Edition, Vol. 28, No. 3. John Wiley & Sons, 2012.
23. Hong, J. and M. J. Lancaster, *Microstrip Filters for RF/Microwave Applications*, Vol. 7. John Wiley & Sons, 2001.
24. Muhsin and R. P. Pudji, "Dual-cross-polarized antenna decoupling for 43 GHz planar massive MIMO in full duplex single channel communications," *Int. J. Adv. Comput. Sci. Appl.*, Vol. 10, No. 4, 364–370, 2019.